BABAR-PUB-05/048
SLAC-PUB-11600

Search for the Rare Decays $B^0 \to D_s^{(*)+} a_{0(2)}^-$

B. Aubert,[1] R. Barate,[1] D. Boutigny,[1] F. Couderc,[1] Y. Karyotakis,[1] J. P. Lees,[1] V. Poireau,[1] V. Tisserand,[1] A. Zghiche,[1] E. Grauges,[2] A. Palano,[3] M. Pappagallo,[3] A. Pompili,[3] J. C. Chen,[4] N. D. Qi,[4] G. Rong,[4] P. Wang,[4] Y. S. Zhu,[4] G. Eigen,[5] I. Ofte,[5] B. Stugu,[5] G. S. Abrams,[6] M. Battaglia,[6] D. Best,[6] A. B. Breon,[6] D. N. Brown,[6] J. Button-Shafer,[6] R. N. Cahn,[6] E. Charles,[6] C. T. Day,[6] M. S. Gill,[6] A. V. Gritsan,[6] Y. Groysman,[6] R. G. Jacobsen,[6] R. W. Kadel,[6] J. Kadyk,[6] L. T. Kerth,[6] Yu. G. Kolomensky,[6] G. Kukartsev,[6] G. Lynch,[6] L. M. Mir,[6] P. J. Oddone,[6] T. J. Orimoto,[6] M. Pripstein,[6] N. A. Roe,[6] M. T. Ronan,[6] W. A. Wenzel,[6] M. Barrett,[7] K. E. Ford,[7] T. J. Harrison,[7] A. J. Hart,[7] C. M. Hawkes,[7] S. E. Morgan,[7] A. T. Watson,[7] M. Fritsch,[8] K. Goetzen,[8] T. Held,[8] H. Koch,[8] B. Lewandowski,[8] M. Pelizaeus,[8] K. Peters,[8] T. Schroeder,[8] M. Steinke,[8] J. T. Boyd,[9] J. P. Burke,[9] W. N. Cottingham,[9] T. Cuhadar-Donszelmann,[10] B. G. Fulsom,[10] C. Hearty,[10] N. S. Knecht,[10] T. S. Mattison,[10] J. A. McKenna,[10] A. Khan,[11] P. Kyberd,[11] M. Saleem,[11] L. Teodorescu,[11] A. E. Blinov,[12] V. E. Blinov,[12] A. D. Bukin,[12] V. P. Druzhinin,[12] V. B. Golubev,[12] E. A. Kravchenko,[12] A. P. Onuchin,[12] S. I. Serednyakov,[12] Yu. I. Skovpen,[12] E. P. Solodov,[12] A. N. Yushkov,[12] M. Bondioli,[13] M. Bruinsma,[13] M. Chao,[13] S. Curry,[13] I. Eschrich,[13] D. Kirkby,[13] A. J. Lankford,[13] P. Lund,[13] M. Mandelkern,[13] R. K. Mommsen,[13] W. Roethel,[13] D. P. Stoker,[13] C. Buchanan,[14] B. L. Hartfiel,[14] S. D. Foulkes,[15] J. W. Gary,[15] O. Long,[15] B. C. Shen,[15] K. Wang,[15] L. Zhang,[15] D. del Re,[16] H. K. Hadavand,[16] E. J. Hill,[16] D. B. MacFarlane,[16] H. P. Paar,[16] S. Rahatlou,[16] V. Sharma,[16] J. W. Berryhill,[17] C. Campagnari,[17] A. Cunha,[17] B. Dahmes,[17] T. M. Hong,[17] M. A. Mazur,[17] J. D. Richman,[17] W. Verkerke,[17] T. W. Beck,[18] A. M. Eisner,[18] C. J. Flacco,[18] C. A. Heusch,[18] J. Kroseberg,[18] W. S. Lockman,[18] G. Nesom,[18] T. Schalk,[18] B. A. Schumm,[18] A. Seiden,[18] P. Spradlin,[18] D. C. Williams,[18] M. G. Wilson,[18] J. Albert,[19] E. Chen,[19] G. P. Dubois-Felsmann,[19] A. Dvoretskii,[19] D. G. Hitlin,[19] J. S. Minamora,[19] I. Narsky,[19] T. Piatenko,[19] F. C. Porter,[19] A. Ryd,[19] A. Samuel,[19] R. Andreassen,[20] G. Mancinelli,[20] B. T. Meadows,[20] M. D. Sokoloff,[20] F. Blanc,[21] P. C. Bloom,[21] S. Chen,[21] W. T. Ford,[21] J. F. Hirschauer,[21] A. Kreisel,[21] U. Nauenberg,[21] A. Olivas,[21] W. O. Ruddick,[21] J. G. Smith,[21] K. A. Ulmer,[21] S. R. Wagner,[21] J. Zhang,[21] A. Chen,[22] E. A. Eckhart,[22] J. L. Harton,[22] A. Soffer,[22] W. H. Toki,[22] R. J. Wilson,[22] F. Winklmeier,[22] Q. Zeng,[22] D. Altenburg,[23] E. Feltresi,[23] A. Hauke,[23] B. Spaan,[23] T. Brandt,[24] J. Brose,[24] M. Dickopp,[24] V. Klose,[24] H. M. Lacker,[24] R. Nogowski,[24] S. Otto,[24] A. Petzold,[24] J. Schubert,[24] K. R. Schubert,[24] R. Schwierz,[24] J. E. Sundermann,[24] D. Bernard,[25] G. R. Bonneaud,[25] P. Grenier,[25] E. Latour,[25] S. Schrenk,[25] Ch. Thiebaux,[25] G. Vasileiadis,[25] M. Verderi,[25] D. J. Bard,[26] P. J. Clark,[26] W. Gradl,[26] F. Muheim,[26] S. Playfer,[26] Y. Xie,[26] M. Andreotti,[27] D. Bettoni,[27] C. Bozzi,[27] R. Calabrese,[27] G. Cibinetto,[27] E. Luppi,[27] M. Negrini,[27] L. Piemontese,[27] F. Anulli,[28] R. Baldini-Ferroli,[28] A. Calcaterra,[28] R. de Sangro,[28] G. Finocchiaro,[28] P. Patteri,[28] I. M. Peruzzi,[28,*] M. Piccolo,[28] A. Zallo,[28] A. Buzzo,[29] R. Capra,[29] R. Contri,[29] M. Lo Vetere,[29] M. M. Macri,[29] M. R. Monge,[29] S. Passaggio,[29] C. Patrignani,[29] E. Robutti,[29] A. Santroni,[29] S. Tosi,[29] G. Brandenburg,[30] K. S. Chaisanguanthum,[30] M. Morii,[30] J. Wu,[30] R. S. Dubitzky,[31] U. Langenegger,[31] J. Marks,[31] S. Schenk,[31] U. Uwer,[31] W. Bhimji,[32] D. A. Bowerman,[32] P. D. Dauncey,[32] U. Egede,[32] R. L. Flack,[32] J. R. Gaillard,[32] J .A. Nash,[32] M. B. Nikolich,[32] W. Panduro Vazquez,[32] X. Chai,[33] M. J. Charles,[33] W. F. Mader,[33] U. Mallik,[33] V. Ziegler,[33] J. Cochran,[34] H. B. Crawley,[34] L. Dong,[34] V. Eyges,[34] W. T. Meyer,[34] S. Prell,[34] E. I. Rosenberg,[34] A. E. Rubin,[34] J. I. Yi,[34] G. Schott,[35] N. Arnaud,[36] M. Davier,[36] X. Giroux,[36] G. Grosdidier,[36] A. Höcker,[36] F. Le Diberder,[36] V. Lepeltier,[36] A. M. Lutz,[36] A. Oyanguren,[36] T. C. Petersen,[36] S. Plaszczynski,[36] S. Rodier,[36] P. Roudeau,[36] M. H. Schune,[36] A. Stocchi,[36] W. Wang,[36] G. Wormser,[36] C. H. Cheng,[37] D. J. Lange,[37] D. M. Wright,[37] A. J. Bevan,[38] C. A. Chavez,[38] I. J. Forster,[38] J. R. Fry,[38] E. Gabathuler,[38] R. Gamet,[38] K. A. George,[38] D. E. Hutchcroft,[38] R. J. Parry,[38] D. J. Payne,[38] K. C. Schofield,[38] C. Touramanis,[38] F. Di Lodovico,[39] W. Menges,[39] R. Sacco,[39] C. L. Brown,[40] G. Cowan,[40] H. U. Flaecher,[40] M. G. Green,[40] D. A. Hopkins,[40] P. S. Jackson,[40] T. R. McMahon,[40] S. Ricciardi,[40] F. Salvatore,[40] D. N. Brown,[41] C. L. Davis,[41] J. Allison,[42] N. R. Barlow,[42] R. J. Barlow,[42] Y. M. Chia,[42] C. L. Edgar,[42] M. C. Hodgkinson,[42] M. P. Kelly,[42] G. D. Lafferty,[42] M. T. Naisbit,[42] J. C. Williams,[42] C. Chen,[43] W. D. Hulsbergen,[43] A. Jawahery,[43] D. Kovalskyi,[43] C. K. Lae,[43] D. A. Roberts,[43] G. Simi,[43] G. Blaylock,[44] C. Dallapiccola,[44] S. S. Hertzbach,[44] R. Kofler,[44] X. Li,[44] T. B. Moore,[44] S. Saremi,[44] H. Staengle,[44] S. Y. Willocq,[44] R. Cowan,[45] K. Koeneke,[45] G. Sciolla,[45]

S. J. Sekula,[45] M. Spitznagel,[45] F. Taylor,[45] R. K. Yamamoto,[45] H. Kim,[46] P. M. Patel,[46] S. H. Robertson,[46] A. Lazzaro,[47] V. Lombardo,[47] F. Palombo,[47] J. M. Bauer,[48] L. Cremaldi,[48] V. Eschenburg,[48] R. Godang,[48] R. Kroeger,[48] J. Reidy,[48] D. A. Sanders,[48] D. J. Summers,[48] H. W. Zhao,[48] S. Brunet,[49] D. Côté,[49] P. Taras,[49] F. B. Viaud,[49] H. Nicholson,[50] N. Cavallo,[51,†] G. De Nardo,[51] F. Fabozzi,[51,†] C. Gatto,[51] L. Lista,[51] D. Monorchio,[51] P. Paolucci,[51] D. Piccolo,[51] C. Sciacca,[51] M. Baak,[52] H. Bulten,[52] G. Raven,[52] H. L. Snoek,[52] L. Wilden,[52] C. P. Jessop,[53] J. M. LoSecco,[53] T. Allmendinger,[54] G. Benelli,[54] K. K. Gan,[54] K. Honscheid,[54] D. Hufnagel,[54] P. D. Jackson,[54] H. Kagan,[54] R. Kass,[54] T. Pulliam,[54] A. M. Rahimi,[54] R. Ter-Antonyan,[54] Q. K. Wong,[54] N. L. Blount,[55] J. Brau,[55] R. Frey,[55] O. Igonkina,[55] M. Lu,[55] C. T. Potter,[55] R. Rahmat,[55] N. B. Sinev,[55] D. Strom,[55] J. Strube,[55] E. Torrence,[55] F. Galeazzi,[56] M. Margoni,[56] M. Morandin,[56] M. Posocco,[56] M. Rotondo,[56] F. Simonetto,[56] R. Stroili,[56] C. Voci,[56] M. Benayoun,[57] J. Chauveau,[57] P. David,[57] L. Del Buono,[57] Ch. de la Vaissière,[57] O. Hamon,[57] M. J. J. John,[57] Ph. Leruste,[57] J. Malclès,[57] J. Ocariz,[57] L. Roos,[57] G. Therin,[57] P. K. Behera,[58] L. Gladney,[58] Q. H. Guo,[58] J. Panetta,[58] M. Biasini,[59] R. Covarelli,[59] S. Pacetti,[59] M. Pioppi,[59] C. Angelini,[60] G. Batignani,[60] S. Bettarini,[60] F. Bucci,[60] G. Calderini,[60] M. Carpinelli,[60] R. Cenci,[60] F. Forti,[60] M. A. Giorgi,[60] A. Lusiani,[60] G. Marchiori,[60] M. Morganti,[60] N. Neri,[60] E. Paoloni,[60] M. Rama,[60] G. Rizzo,[60] J. Walsh,[60] M. Haire,[61] D. Judd,[61] D. E. Wagoner,[61] J. Biesiada,[62] N. Danielson,[62] P. Elmer,[62] Y. P. Lau,[62] C. Lu,[62] J. Olsen,[62] A. J. S. Smith,[62] A. V. Telnov,[62] F. Bellini,[63] G. Cavoto,[63] A. D'Orazio,[63] E. Di Marco,[63] R. Faccini,[63] F. Ferrarotto,[63] F. Ferroni,[63] M. Gaspero,[63] L. Li Gioi,[63] M. A. Mazzoni,[63] S. Morganti,[63] G. Piredda,[63] F. Polci,[63] F. Safai Tehrani,[63] C. Voena,[63] H. Schröder,[64] R. Waldi,[64] T. Adye,[65] N. De Groot,[65] B. Franek,[65] G. P. Gopal,[65] E. O. Olaiya,[65] F. F. Wilson,[65] R. Aleksan,[66] S. Emery,[66] A. Gaidot,[66] S. F. Ganzhur,[66] G. Graziani,[66] G. Hamel de Monchenault,[66] W. Kozanecki,[66] M. Legendre,[66] G. W. London,[66] B. Mayer,[66] G. Vasseur,[66] Ch. Yèche,[66] M. Zito,[66] M. V. Purohit,[67] A. W. Weidemann,[67] J. R. Wilson,[67] T. Abe,[68] M. T. Allen,[68] D. Aston,[68] R. Bartoldus,[68] N. Berger,[68] A. M. Boyarski,[68] O. L. Buchmueller,[68] R. Claus,[68] J. P. Coleman,[68] M. R. Convery,[68] M. Cristinziani,[68] J. C. Dingfelder,[68] D. Dong,[68] J. Dorfan,[68] D. Dujmic,[68] W. Dunwoodie,[68] S. Fan,[68] R. C. Field,[68] T. Glanzman,[68] S. J. Gowdy,[68] T. Hadig,[68] V. Halyo,[68] C. Hast,[68] T. Hryn'ova,[68] W. R. Innes,[68] M. H. Kelsey,[68] P. Kim,[68] M. L. Kocian,[68] D. W. G. S. Leith,[68] J. Libby,[68] S. Luitz,[68] V. Luth,[68] H. L. Lynch,[68] H. Marsiske,[68] R. Messner,[68] D. R. Muller,[68] C. P. O'Grady,[68] V. E. Ozcan,[68] A. Perazzo,[68] M. Perl,[68] B. N. Ratcliff,[68] A. Roodman,[68] A. A. Salnikov,[68] R. H. Schindler,[68] J. Schwiening,[68] A. Snyder,[68] J. Stelzer,[68] D. Su,[68] M. K. Sullivan,[68] K. Suzuki,[68] S. K. Swain,[68] J. M. Thompson,[68] J. Va'vra,[68] N. van Bakel,[68] M. Weaver,[68] A. J. R. Weinstein,[68] W. J. Wisniewski,[68] M. Wittgen,[68] D. H. Wright,[68] A. K. Yarritu,[68] K. Yi,[68] C. C. Young,[68] P. R. Burchat,[69] A. J. Edwards,[69] S. A. Majewski,[69] B. A. Petersen,[69] C. Roat,[69] M. Ahmed,[70] S. Ahmed,[70] M. S. Alam,[70] R. Bula,[70] J. A. Ernst,[70] M. A. Saeed,[70] F. R. Wappler,[70] S. B. Zain,[70] W. Bugg,[71] M. Krishnamurthy,[71] S. M. Spanier,[71] R. Eckmann,[72] J. L. Ritchie,[72] A. Satpathy,[72] R. F. Schwitters,[72] J. M. Izen,[73] I. Kitayama,[73] X. C. Lou,[73] S. Ye,[73] F. Bianchi,[74] M. Bona,[74] F. Gallo,[74] D. Gamba,[74] M. Bomben,[75] L. Bosisio,[75] C. Cartaro,[75] F. Cossutti,[75] G. Della Ricca,[75] S. Dittongo,[75] S. Grancagnolo,[75] L. Lanceri,[75] L. Vitale,[75] V. Azzolini,[76] F. Martinez-Vidal,[76] R. S. Panvini,[77,‡] Sw. Banerjee,[78] B. Bhuyan,[78] C. M. Brown,[78] D. Fortin,[78] K. Hamano,[78] R. Kowalewski,[78] I. M. Nugent,[78] J. M. Roney,[78] R. J. Sobie,[78] J. J. Back,[79] P. F. Harrison,[79] T. E. Latham,[79] G. B. Mohanty,[79] H. R. Band,[80] X. Chen,[80] B. Cheng,[80] S. Dasu,[80] M. Datta,[80] A. M. Eichenbaum,[80] K. T. Flood,[80] M. T. Graham,[80] J. J. Hollar,[80] J. R. Johnson,[80] P. E. Kutter,[80] H. Li,[80] R. Liu,[80] B. Mellado,[80] A. Mihalyi,[80] A. K. Mohapatra,[80] Y. Pan,[80] M. Pierini,[80] R. Prepost,[80] P. Tan,[80] S. L. Wu,[80] Z. Yu,[80] and H. Neal[81]

(The *BABAR* Collaboration)

[1]*Laboratoire de Physique des Particules, F-74941 Annecy-le-Vieux, France*
[2]*IFAE, Universitat Autonoma de Barcelona, E-08193 Bellaterra, Barcelona, Spain*
[3]*Università di Bari, Dipartimento di Fisica and INFN, I-70126 Bari, Italy*
[4]*Institute of High Energy Physics, Beijing 100039, China*
[5]*University of Bergen, Institute of Physics, N-5007 Bergen, Norway*
[6]*Lawrence Berkeley National Laboratory and University of California, Berkeley, California 94720, USA*
[7]*University of Birmingham, Birmingham, B15 2TT, United Kingdom*
[8]*Ruhr Universität Bochum, Institut für Experimentalphysik 1, D-44780 Bochum, Germany*
[9]*University of Bristol, Bristol BS8 1TL, United Kingdom*
[10]*University of British Columbia, Vancouver, British Columbia, Canada V6T 1Z1*
[11]*Brunel University, Uxbridge, Middlesex UB8 3PH, United Kingdom*
[12]*Budker Institute of Nuclear Physics, Novosibirsk 630090, Russia*
[13]*University of California at Irvine, Irvine, California 92697, USA*

[14] University of California at Los Angeles, Los Angeles, California 90024, USA
[15] University of California at Riverside, Riverside, California 92521, USA
[16] University of California at San Diego, La Jolla, California 92093, USA
[17] University of California at Santa Barbara, Santa Barbara, California 93106, USA
[18] University of California at Santa Cruz, Institute for Particle Physics, Santa Cruz, California 95064, USA
[19] California Institute of Technology, Pasadena, California 91125, USA
[20] University of Cincinnati, Cincinnati, Ohio 45221, USA
[21] University of Colorado, Boulder, Colorado 80309, USA
[22] Colorado State University, Fort Collins, Colorado 80523, USA
[23] Universität Dortmund, Institut für Physik, D-44221 Dortmund, Germany
[24] Technische Universität Dresden, Institut für Kern- und Teilchenphysik, D-01062 Dresden, Germany
[25] Ecole Polytechnique, LLR, F-91128 Palaiseau, France
[26] University of Edinburgh, Edinburgh EH9 3JZ, United Kingdom
[27] Università di Ferrara, Dipartimento di Fisica and INFN, I-44100 Ferrara, Italy
[28] Laboratori Nazionali di Frascati dell'INFN, I-00044 Frascati, Italy
[29] Università di Genova, Dipartimento di Fisica and INFN, I-16146 Genova, Italy
[30] Harvard University, Cambridge, Massachusetts 02138, USA
[31] Universität Heidelberg, Physikalisches Institut, Philosophenweg 12, D-69120 Heidelberg, Germany
[32] Imperial College London, London, SW7 2AZ, United Kingdom
[33] University of Iowa, Iowa City, Iowa 52242, USA
[34] Iowa State University, Ames, Iowa 50011-3160, USA
[35] Universität Karlsruhe, Institut für Experimentelle Kernphysik, D-76021 Karlsruhe, Germany
[36] Laboratoire de l'Accélérateur Linéaire, F-91898 Orsay, France
[37] Lawrence Livermore National Laboratory, Livermore, California 94550, USA
[38] University of Liverpool, Liverpool L69 72E, United Kingdom
[39] Queen Mary, University of London, E1 4NS, United Kingdom
[40] University of London, Royal Holloway and Bedford New College, Egham, Surrey TW20 0EX, United Kingdom
[41] University of Louisville, Louisville, Kentucky 40292, USA
[42] University of Manchester, Manchester M13 9PL, United Kingdom
[43] University of Maryland, College Park, Maryland 20742, USA
[44] University of Massachusetts, Amherst, Massachusetts 01003, USA
[45] Massachusetts Institute of Technology, Laboratory for Nuclear Science, Cambridge, Massachusetts 02139, USA
[46] McGill University, Montréal, Québec, Canada H3A 2T8
[47] Università di Milano, Dipartimento di Fisica and INFN, I-20133 Milano, Italy
[48] University of Mississippi, University, Mississippi 38677, USA
[49] Université de Montréal, Physique des Particules, Montréal, Québec, Canada H3C 3J7
[50] Mount Holyoke College, South Hadley, Massachusetts 01075, USA
[51] Università di Napoli Federico II, Dipartimento di Scienze Fisiche and INFN, I-80126, Napoli, Italy
[52] NIKHEF, National Institute for Nuclear Physics and High Energy Physics, NL-1009 DB Amsterdam, The Netherlands
[53] University of Notre Dame, Notre Dame, Indiana 46556, USA
[54] Ohio State University, Columbus, Ohio 43210, USA
[55] University of Oregon, Eugene, Oregon 97403, USA
[56] Università di Padova, Dipartimento di Fisica and INFN, I-35131 Padova, Italy
[57] Universités Paris VI et VII, Laboratoire de Physique Nucléaire et de Hautes Energies, F-75252 Paris, France
[58] University of Pennsylvania, Philadelphia, Pennsylvania 19104, USA
[59] Università di Perugia, Dipartimento di Fisica and INFN, I-06100 Perugia, Italy
[60] Università di Pisa, Dipartimento di Fisica, Scuola Normale Superiore and INFN, I-56127 Pisa, Italy
[61] Prairie View A&M University, Prairie View, Texas 77446, USA
[62] Princeton University, Princeton, New Jersey 08544, USA
[63] Università di Roma La Sapienza, Dipartimento di Fisica and INFN, I-00185 Roma, Italy
[64] Universität Rostock, D-18051 Rostock, Germany
[65] Rutherford Appleton Laboratory, Chilton, Didcot, Oxon, OX11 0QX, United Kingdom
[66] DSM/Dapnia, CEA/Saclay, F-91191 Gif-sur-Yvette, France
[67] University of South Carolina, Columbia, South Carolina 29208, USA
[68] Stanford Linear Accelerator Center, Stanford, California 94309, USA
[69] Stanford University, Stanford, California 94305-4060, USA
[70] State University of New York, Albany, New York 12222, USA
[71] University of Tennessee, Knoxville, Tennessee 37996, USA
[72] University of Texas at Austin, Austin, Texas 78712, USA
[73] University of Texas at Dallas, Richardson, Texas 75083, USA
[74] Università di Torino, Dipartimento di Fisica Sperimentale and INFN, I-10125 Torino, Italy
[75] Università di Trieste, Dipartimento di Fisica and INFN, I-34127 Trieste, Italy
[76] IFIC, Universitat de Valencia-CSIC, E-46071 Valencia, Spain
[77] Vanderbilt University, Nashville, Tennessee 37235, USA

[78] University of Victoria, Victoria, British Columbia, Canada V8W 3P6
[79] Department of Physics, University of Warwick, Coventry CV4 7AL, United Kingdom
[80] University of Wisconsin, Madison, Wisconsin 53706, USA
[81] Yale University, New Haven, Connecticut 06511, USA

(Dated: February 7, 2008)

We have searched for the decays $B^0 \to D_s^+ a_0^-$, $B^0 \to D_s^{*+} a_0^-$, $B^0 \to D_s^+ a_2^-$ and $B^0 \to D_s^{*+} a_2^-$ in a sample of about 230 million $\Upsilon(4S) \to B\overline{B}$ decays collected with the *BABAR* detector at the PEP-II asymmetric-energy B Factory at SLAC. We find no evidence for these decays and set upper limits at 90% C.L. on the branching fractions: $\mathcal{B}(B^0 \to D_s^+ a_0^-) < 1.9 \times 10^{-5}$, $\mathcal{B}(B^0 \to D_s^{*+} a_0^-) < 3.6 \times 10^{-5}$, $\mathcal{B}(B^0 \to D_s^+ a_2^-) < 1.9 \times 10^{-4}$, and $\mathcal{B}(B^0 \to D_s^{*+} a_2^-) < 2.0 \times 10^{-4}$.

PACS numbers: 13.25.Hw, 12.15.Hh, 11.30.Er

The time-dependent decay rates for neutral B mesons into a D meson and a light meson provide sensitivity to the Cabibbo-Kobayashi-Maskawa (CKM) [1] quark mixing matrix phases β and γ [2]. A *CP*-violating term emerges through the interference between $B^0\overline{B}^0$ mixing mediated and direct decay amplitudes. The time-dependent *CP*-asymmetries in the decay modes $B^0 \to D^{(*)-}\pi^+$ [3] have been studied by *BABAR* and BELLE [4, 5]. In these modes, the *CP*-asymmetries arise due to a phase difference between two amplitudes of very different magnitudes: one decay amplitude is suppressed by the product of two small CKM elements V_{ub} and V_{cd}, while the other is CKM favored. Therefore, the decay rate is dominated by the CKM-favored part of the amplitude, resulting in a very small *CP*-violating asymmetry.

Recently it was proposed to consider other types of light mesons in the two-body final states [6]. The idea is that decay amplitudes with light scalar or tensor mesons, such as a_0^+ or a_2^+, emitted from a weak current, are significantly suppressed because of the small coupling constants $f_{a_{0(2)}}$. In the $SU(2)$ limit, $f_{a_0} = 0$ (since the coupling constant of a light scalar is proportional to the mass difference between u and d quarks), and any non-zero value of f_{a_0} is of the order of isospin conservation breaking effects. Since the light tensor meson a_2^+ has spin 2, it cannot be emitted by a W-boson (i.e. $f_{a_2} \equiv 0$), and thus could only appear in a V_{cb}-mediated process via final state hadronic interactions and rescattering. Therefore, the absolute values of the CKM-suppressed and favored parts of the decay amplitude (see Figure 1, top two diagrams) could become comparable, potentially resulting in a large *CP*-asymmetry. No $B \to a_{0(2)}X$ transitions have been observed yet. A summary of the theoretical predictions for the values of V_{ub} and V_{cb}-mediated parts of the $B^0 \to D^{(*)-}a_{0(2)}^+$ branching fractions can be found in [7].

The V_{ub}-mediated amplitudes in [7] were computed in the factorization framework. In addition to model uncertainties, significant uncertainty in the theoretical calculations is due to unknown $B \to a_{0(2)}X$ transition form factors. One way to verify the numerical assumptions and test the validity of the factorization approach experimentally is to measure the branching fractions for the $SU(3)$ conjugated decay modes $B^0 \to D_s^{(*)+}a_{0(2)}$. These decays are represented by a single tree diagram (Figure 1, bottom diagram) with external W^+ emission, without contributions from additional tree or penguin diagrams. The V_{ub}-mediated part of the $B^0 \to D^{(*)+}a_{0(2)}^-$ decay amplitude can be related to $B^0 \to D_s^{(*)+}a_{0(2)}^-$ using $\tan(\theta_{\rm Cabibbo}) = |V_{cd}/V_{cs}|$ and the ratio of the decay constants $f_{D_s^{(*)}}/f_{D^{(*)}}$.

Branching fractions of $B^0 \to D_s^{(*)+}a_2^-$ are predicted to be in the range 1.3–1.8 (2.1–2.9) in units of 10^{-5} [8]. Branching fraction estimates for $B^0 \to D_s^{(*)+}a_0^-$ of approximately 8×10^{-5} are obtained using $SU(3)$ symmetry from the predictions made for $B^0 \to D^{(*)+}a_0^-$ in [7].

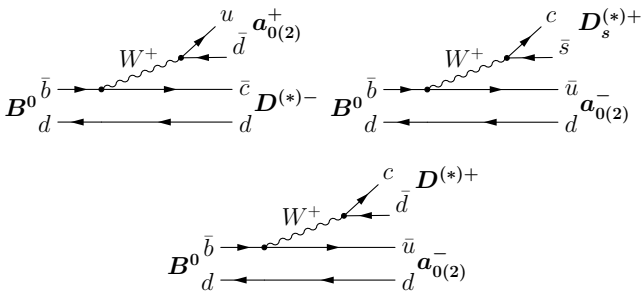

FIG. 1: Top diagrams: tree diagrams contributing to the decay amplitude of $B^0 \to D^{(*)-}a_{0(2)}^+$ (including the $B^0\overline{B}^0$ mixing mediated part of the amplitude). Bottom diagram: tree diagram representing the decay amplitude of $B^0 \to D_s^{(*)+}a_{0(2)}^-$.

In this paper we present the first search for the decays $B^0 \to D_s^+ a_0^-$, $B^0 \to D_s^{*+} a_0^-$, $B^0 \to D_s^+ a_2^-$ and $B^0 \to D_s^{*+} a_2^-$. The analysis uses a sample of approximately 210 fb^{-1}, which corresponds to about 230 million $\Upsilon(4S)$ decays into $B\overline{B}$ pairs collected in the years 1999–2004 with the *BABAR* detector at the asymmetric-energy B-factory PEP-II [9]. The *BABAR* detector is described elsewhere [10] and only the components crucial to this analysis are summarized here. Charged particle

tracking is provided by a five-layer silicon vertex tracker (SVT) and a 40-layer drift chamber (DCH). For charged-particle identification, ionization energy loss (dE/dx) in the DCH and SVT, and Cherenkov radiation detected in a ring-imaging device are used. Photons are identified and measured using the electromagnetic calorimeter, which is comprised of 6580 thallium-doped CsI crystals. These systems are located inside a 1.5 T solenoidal superconducting magnet. We use GEANT4 [11] software to simulate interactions of particles traversing the *BABAR* detector, taking into account the varying detector conditions and beam backgrounds.

The selection criteria are optimized by maximizing the ratio of expected signal events S to the square-root of the sum of signal and background events B. For the calculation of S we assume $\mathcal{B}(B^0 \to D_s^{(*)+} a_2^-)$ to be the mean values of the predicted intervals from [8] and an estimate of $\mathcal{B}(B^0 \to D_s^{(*)+} a_0^-)$ is obtained from $\mathcal{B}(B^0 \to D^{(*)+} a_0^-)$ predicted in [7] and assuming $SU(3)$ symmetry. The optimal selection criteria as well as the shapes of the distributions of selection variables are determined from simulated Monte Carlo (MC) events. We use MC samples of our signal modes and, to simulate background, inclusive samples of B^+B^- (800 fb^{-1}), $B^0\overline{B}^0$ (782 fb^{-1}), $c\bar{c}$ (263 fb^{-1}), and $q\bar{q}$, $q = u, d, s$ (279 fb^{-1}). In addition, we use large samples of simulated events of rare background modes which have final states similar to the signal.

Candidates for D_s^+ mesons are reconstructed in the modes $D_s^+ \to \phi\pi^+$, $\overline{K}^{*0}K^+$, and $K_S^0K^+$, with $\phi \to K^+K^-$, $\overline{K}^{*0} \to K^-\pi^+$ and $K_S^0 \to \pi^+\pi^-$. The K_S^0 candidates are reconstructed from two oppositely-charged tracks, with an invariant mass close to the nominal K_S^0 mass [12], that come from a common vertex displaced from the e^+e^- interaction point. All other tracks are required to originate less than 1.5 cm away from the e^+e^- interaction point in the transverse plane and less than 10 cm along the beam axis. Charged kaon candidates must satisfy kaon identification criteria that are typically around 95% efficient, depending on momentum and polar angle, and have a misidentification rate at the 10% level. The $\phi \to K^+K^-$, $\overline{K}^{*0} \to K^-\pi^+$ and $K_S^0 \to \pi^+\pi^-$ candidates are required to have invariant masses close to their nominal masses [12] (we require the absolute differences between their measured masses and the nominal values [12] to be in the range 12–15 MeV, 35–60 MeV and 7–12 MeV, respectively, depending on the B^0 and D_s^+ decay modes). The polarizations of the $\overline{K}^{*0}$ and ϕ mesons in the D_s^+ decays are used to reject backgrounds through the use of the helicity angle θ_H, defined as the angle between the K^- momentum vector and the direction of flight of the D_s^+ in the $\overline{K}^{*0}$ or ϕ rest frame. The $\overline{K}^{*0}$ candidates are required to have $|\cos\theta_H|$ greater than 0.25–0.5 and ϕ candidates are required to have $|\cos\theta_H|$ greater than 0.3–0.5, depending on the B^0 decay mode. We also apply a vertex fit to the D_s^+ candidates that decay into $\phi\pi^+$ and $\overline{K}^{*0}K^+$, since all charged daughter tracks of D_s^+ are supposed to come from a common vertex. The χ^2 of the vertex fit is required to be less than 10–16 (which corresponds to a probability of better than $0.1\% - 1.9\%$ for the 3 track vertex fit), depending on the reconstructed mode.

The D_s^{*+} candidates are reconstructed in the mode $D_s^{*+} \to D_s^+\gamma$. The photons are required to have an energy greater than 100 MeV. The D_s^+ and D_s^{*+} candidates are required to have invariant masses less than about $\pm 2\sigma$ from their nominal values [12]. The invariant mass of the D_s^{*+} is calculated after the mass constraint on the daughter D_s^+ has been applied. Subsequently, all D_s^{*+} candidates are subjected to a mass-constrained fit.

We reconstruct a_0^- and a_2^- candidates in their decay to the $\eta\pi^-$ final state. For reconstructed $\eta \to \gamma\gamma$ candidates we require the energy of each photon to be greater than 250 MeV for a_0^+ candidates, and greater than 300 – 400 MeV for a_2^+ candidates, depending on the D_s^+ mode. The η mass is required to be within a $\pm 1\sigma$ or $\pm 2\sigma$ interval of the nominal value [12], depending on the background conditions in a particular B^0, D_s^+ decay mode (the η mass resolution is measured to be around 15 MeV/c^2). The a_0^+ and a_2^+ candidates are required to have a mass $m_{\eta\pi^+}$ in the range 0.9–1.1 GeV/c^2 and 1.2–1.5 GeV/c^2, respectively. We also require that photons from η and D_s^{*+} are inconsistent with π^0 hypothesis when combined with any other photon in the event (the π^0 veto window varies from ± 10 to ± 15 MeV/c^2). Finally, the B^0 meson candidates are formed using the reconstructed combinations of $D_s^+a_0^-$, $D_s^+a_2^-$, $D_s^{*+}a_0^-$ and $D_s^{*+}a_2^-$.

The background from continuum $q\bar{q}$ production (where $q = u, d, s, c$) is suppressed based on the event topology. We calculate the angle (θ_T) between the thrust axis of the B meson candidate and the thrust axis of all other particles in the event. In the center-of-mass frame (c.m.), $B\overline{B}$ pairs are produced approximately at rest and have a uniform $\cos\theta_T$ distribution. In contrast, $q\bar{q}$ pairs are produced in the c.m. frame with high momentum, which results in a $|\cos\theta_T|$ distribution peaking at 1. Depending on the background level of each mode, $|\cos\theta_T|$ is required to be smaller than 0.70–0.75. We further suppress backgrounds using a Fisher discriminant ($\mathcal{F}$) [13] constructed from the scalar sum of the c.m. momenta of all tracks and photons (excluding the B candidate decay products) flowing into 9 concentric cones centered on the thrust axis of the B candidate. The more isotropic the event, the larger the value of $\mathcal{F}$. We require $\mathcal{F}$ to be larger than a threshold that retains 75% to 86% of the signal while rejecting 78% to 65% of the background, depending on the background level. In addition, the ratio of the second and zeroth order Fox-Wolfram moments [14] must be less than a threshold in the range 0.25–0.40 depending on the decay mode.

We extract the signal using the kinematical variables $m_{\rm ES} = \sqrt{E_{\rm b}^{*2} - (\sum_i \mathbf{p}_i^*)^2}$ and $\Delta E = \sum_i \sqrt{m_i^2 + \mathbf{p}_i^{*2}} -$

$E^*_{\rm b}$, where $E^*_{\rm b}$ is the beam energy in the c.m. frame, $\mathbf{p}^*_i$ is the c.m. momentum of the daughter particle i of the B^0 meson candidate, and m_i is the mass hypothesis for particle i. For signal events, $m_{\rm ES}$ peaks at the B^0 meson mass with a resolution of about 2.7 MeV/c^2 and ΔE peaks near zero with a resolution of 20 MeV, indicating that the B^0 candidate has a total energy consistent with the beam energy in the c.m. frame. The B^0 candidates are required to have $|\Delta E| < 40$ MeV and $m_{\rm ES} > 5.2$ GeV/c^2.

The fraction of multiple B^0 candidates per event is estimated using the MC simulation and found to be around 2% for $D_s^+ a_{0(2)}^-$ and 5% for $D_s^{*+} a_{0(2)}^-$ combinations. In each event with more than one B^0 candidate that passed the selection requirements, we select the one with the lowest $|\Delta E|$ value.

After all selection criteria are applied, we estimate the B^0 reconstruction efficiencies, excluding the intermediate branching fractions (see Table I).

TABLE I: Reconstruction efficiencies for $B^0 \to D_s^{(*)+} a_{0(2)}^-$ decays (excluding the intermediate branching fractions).

Decay mode	$D_s^+ \to \phi\pi^+$	$D_s^+ \to \overline{K}^{*0}K^+$	$D_s^+ \to K_S^0 K^+$
$B^0 \to D_s^+ a_0^-$	4.7%	2.9%	2.5%
$B^0 \to D_s^+ a_2^-$	1.9%	1.1%	1.1%
$B^0 \to D_s^{*+} a_0^-$	2.2%	1.5%	1.3%
$B^0 \to D_s^{*+} a_2^-$	0.9%	0.7%	0.5%

Background events that pass these selection criteria are mostly from $q\bar{q}$ continuum, and their $m_{\rm ES}$ distribution is described by a threshold function [15]:

$$f(m_{\rm ES}) \sim m_{\rm ES}\sqrt{1-x^2}\exp[-\xi(1-x^2)],$$

where $x = 2m_{\rm ES}/\sqrt{s}$, $\sqrt{s}$ is the total energy of the beams in their center of mass frame, and ξ is the fit parameter. A study using simulated events of B^0 and B^+ decay modes with final states similar to our signal mode, including $D_s^{(*)+}\pi^-$ and $D_s^{(*)+}\rho^-$, shows that these modes do not peak in $m_{\rm ES}$.

Figure 2 shows the $m_{\rm ES}$ distributions for the reconstructed candidates $B^0 \to D_s^+ a_0^-$, $B^0 \to D_s^+ a_2^-$, $B^0 \to D_s^{*+} a_0^-$ and $B^0 \to D_s^{*+} a_2^-$. For each mode, we perform an unbinned maximum-likelihood fit to the $m_{\rm ES}$ distributions using the candidates from all D_s^+ decay modes combined. We fit the $m_{\rm ES}$ distributions with the sum of the function $f(m_{ES})$ characterizing the combinatorial background and a Gaussian function to describe the signal. The total signal yield in each B^0 decay mode is calculated as a sum over D_s^+ modes ($i = \phi\pi^+$, $\overline{K}^{*0}K^+$, $K_S^0 K^+$):

$$n_{sig} = \mathcal{B} \cdot N_{B\bar{B}} \cdot \sum_i \mathcal{B}_i \cdot \epsilon_i,$$

where $\mathcal{B}$ is the branching fraction of the B^0 decay mode, $N_{B\bar{B}}$ is the number of produced $B\bar{B}$ pairs, $\mathcal{B}_i$ is the product of the intermediate branching ratios and ϵ_i is the reconstruction efficiency. The mean and the width of the Gaussian function are fixed to values obtained from simulated signal events for each decay mode. The threshold shape parameter ξ, along with the branching ratio $\mathcal{B}$ are free parameters of the fit. The likelihood function is given by:

$$\mathcal{L} = \frac{e^{-N}}{N!}\prod_{i=1}^{N}(n_{sig}P_i^{sig} + (N - n_{sig})P_i^{bkg}),$$

where P_i^{sig} and P_i^{bkg} are the probability density functions for the corresponding hypotheses, N is the total number of events in the fit and i is the index over all events in the fit.

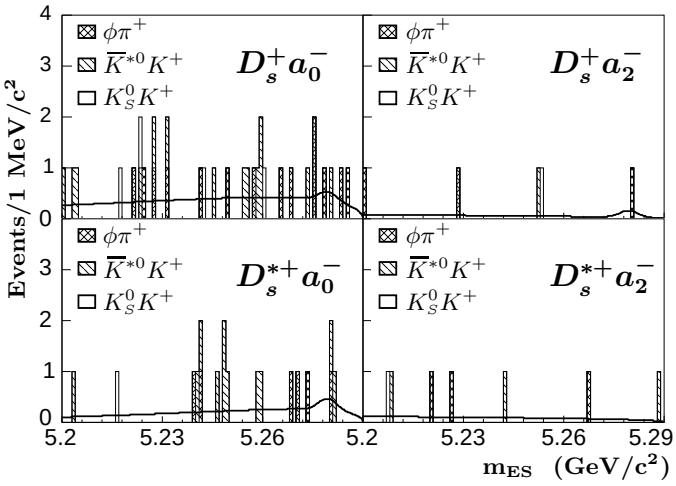

FIG. 2: Distributions of $m_{\rm ES}$ for $B^0 \to D_s^{(*)+} a_{0(2)}^-$ candidates overlaid with the projection of the maximum likelihood fit. Contributions from D_s^+ modes are shown with a different hatching style. The fit procedure and results are described in the text.

Table II (second column) shows the signal event yields from the $m_{\rm ES}$ fit. Due to a lack of entries in the signal region for the $B^0 \to D_s^{*+} a_2^-$ mode, the fit did not yield any central value for the number of signal events in this mode. Accounting for the estimated reconstruction efficiencies and daughter particles branching fractions, we measure the branching fractions shown in the third column of Table II.

The systematic errors include a 14% relative uncertainty for D_s^+ decay rates [16]. Uncertainties in the $m_{\rm ES}$ signal and background shapes result in 11% relative error in the measured branching fractions. The rest of the systematic error sources, which include uncertainties in photon and η reconstruction efficiencies, the a_0^+ and a_2^+ masses and widths, track and K_S^0 reconstruction, charged

TABLE II: Signal yields, branching fractions and upper limits on the branching fractions for $B^0 \to D_s^{(*)+} a_{0(2)}^-$ decays. Numbers in parentheses in the third and fourth columns indicate the branching fractions and the upper limits multiplied by the branching fractions of the decays $D_s^+ \to \phi\pi^+$ and $a_{0(2)}^+ \to \eta\pi^+$.

B^0 mode	n_{sig}	$\mathcal{B}$ $[10^{-5}(10^{-7})]$	$U.L.$ $[10^{-5}]$
$D_s^+ a_0^-$	$0.9^{+2.2}_{-1.7}$	$0.6^{+1.4}_{-1.1} \pm 0.1$ $(2.6^{+6.6}_{-5.1} \pm 0.5)$	1.9 (0.09)
$D_s^+ a_2^-$	$0.6^{+1.0}_{-0.6}$	$6.4^{+10.4}_{-5.7} \pm 1.5$ $(4.5^{+7.3}_{-4.0} \pm 0.8)$	19 (0.13)
$D_s^{*+} a_0^-$	$1.5^{+2.3}_{-1.8}$	$1.4^{+2.1}_{-1.6} \pm 0.3$ $(6.5^{+10.1}_{-7.8} \pm 1.2)$	3.6 (0.17)
$D_s^{*+} a_2^-$	–	– (–)	20 (0.13)

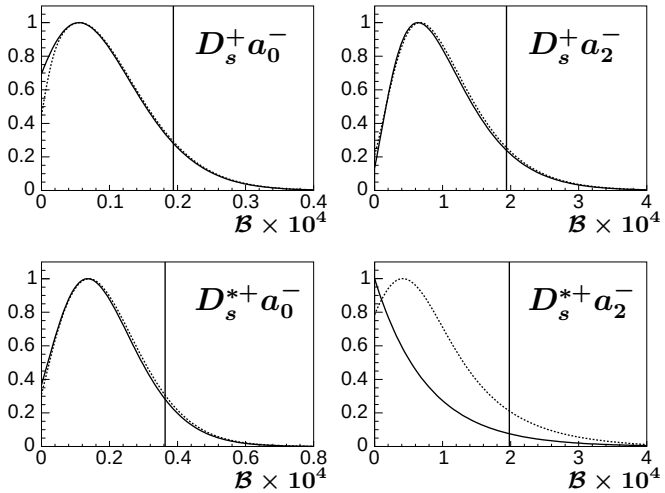

FIG. 3: Likelihood functions of the fit for the $m_{\rm ES}$ distributions of the selected $B^0 \to D_s^{(*)+} a_{0(2)}^-$ candidates. Solid curves represent the original likelihood scan from the fit, the dashed lines show the result of the convolution with the systematic errors Gaussian. Vertical lines indicate the 90% Bayesian C.L. upper limit value.

kaon identification, range between 3% and 10%. We assume the branching fraction for $a_0^+ \to \eta\pi^+$ to be 100% and assign an asymmetric systematic error of -10% to this assumption. The systematic error in the number of produced $B\overline{B}$ pairs is 1.1%. It was checked that the selection of the best candidate based on $|\Delta E|$ does not introduce any significant bias in the m_{ES} fit. The total relative systematic errors are estimated to be around 25% for each mode.

We use a Bayesian approach with a flat prior above zero to set 90% confidence level upper limits on the branching fractions. In a given mode, the upper limit on the branching fraction ($\mathcal{B}_{UL}$) is defined by:

$$\int_0^{\mathcal{B}_{UL}} \mathcal{L}(\mathcal{B}) d\mathcal{B} = 0.9 \times \int_0^{\infty} \mathcal{L}(\mathcal{B}) d\mathcal{B}$$

where $\mathcal{L}(\mathcal{B})$ is the likelihood as a function of the branching fraction $\mathcal{B}$ as determined from the $m_{\rm ES}$ fit described above. We account for systematic uncertainties by numerically convolving $\mathcal{L}(\mathcal{B})$ with a Gaussian distribution with a width determined by the relative systematic uncertainty multiplied by the branching fraction obtained from the $m_{\rm ES}$ fit. In cases with asymmetric errors we took the larger for the width of this Gaussian function. In case of $D_s^{*+} a_2^-$ (where no central value was determined from the fit) we conservatively estimate the absolute systematic error by taking the numerically calculated 90% confidence level upper limit (without the systematic uncertainties) instead of the fitted branching fraction. The resulting upper limits are summarized in Table II (fourth column). The likelihood curves are shown in Figure 3.

We have also calculated upper limits without including the intermediate branching fractions of the decays $D_s^+ \to \phi\pi^+$ [16] and $a_{0(2)}^+ \to \eta\pi^+$ [12]. The relative systematic errors in this case are reduced to 18% for each of the B^0 meson decay modes. The results are presented in Table II (third and fourth columns, numbers in parenthesis).

In conclusion, we do not observe any evidence for the decays $B^0 \to D_s^+ a_0^-$, $B^0 \to D_s^+ a_2^-$, $B^0 \to D_s^{*+} a_0^-$ and $B^0 \to D_s^{*+} a_2^-$, and set 90% C.L. upper limits on their branching fractions. The upper limit value for $B^0 \to D_s^+ a_0^-$ is lower than the theoretical expectation, which might indicate the need to revisit the $B \to a_0 X$ transition form factor estimate. It might also imply the limited applicability of the factorization approach for this decay mode. The upper limits suggest that the branching ratios of $B^0 \to D^{(*)+} a_{0(2)}^-$ are too small for CP-asymmetry measurements given the present statistics of the B-factories.

We are grateful for the excellent luminosity and machine conditions provided by our PEP-II colleagues, and for the substantial dedicated effort from the computing organizations that support *BABAR*. The collaborating institutions wish to thank SLAC for its support and kind hospitality. This work is supported by DOE and NSF (USA), NSERC (Canada), IHEP (China), CEA and CNRS-IN2P3 (France), BMBF and DFG (Germany), INFN (Italy), FOM (The Netherlands), NFR (Norway), MIST (Russia), and PPARC (United Kingdom). Individuals have received support from CONACyT (Mexico), A. P. Sloan Foundation, Research Corporation, and Alexander von Humboldt Foundation.

* Also with Università di Perugia, Dipartimento di Fisica, Perugia, Italy
† Also with Università della Basilicata, Potenza, Italy
‡ Deceased

[1] M. Kobayashi, T. Maskawa, Prog. Theor. Phys. **49**, 652

(1973), N. Cabibbo, Phys. Rev. Lett. **10**, 531 (1963).
[2] $\beta = \arg(-V_{cd}V_{cb}^*/V_{td}V_{tb}^*)$, $\gamma = \arg(-V_{ud}V_{ub}^*/V_{cd}V_{cb}^*)$
[3] Charge conjugate reactions are implicitly included, throughout this paper.
[4] *BABAR* Collaboration, B. Aubert *et al.*, Phys. Rev. Lett. **92**, 251801 (2004); *BABAR* Collaboration, B. Aubert *et al.*, Phys. Rev. Lett. **92**, 251802 (2004);
[5] BELLE Collaboration, K. Abe *al.*, hep-ex/0408106.
[6] M. Diehl, G. Hiller, Phys. Lett. **B 517**, 125 (2001).
[7] M. Diehl, G. Hiller, JHEP 0106:067 (2001).
[8] C.S. Kim, J.P. Lee, and S. Oh, Phys. Rev. **D 67**, 014011 (2003).
[9] PEP-II Conceptual Design Report, SLAC-0418 (1993).
[10] *BABAR* Collaboration, B. Aubert *et al.*, Nucl. Instrum. Methods Phys. Res., Sect. A **479**, 1 (2002).
[11] Geant4 Collaboration, S. Agostinelli *et al.*, Nucl. Instrum. Methods Phys. Res., Sect. A **506**, 250 (2003).
[12] Particle Data Group, S. Eidelman *et al.*, Phys. Lett. **B 592**, 1 (2004).
[13] R.A. Fisher, Annals of Eugenics 7 Part II, 179 (1936).
[14] G.C. Fox and S. Wolfram, Phys. Rev. Lett. **41**, 1581 (1978).
[15] ARGUS Collaboration, H. Albrecht *et al.*, Z. Phys. C **48**, 543 (1990).
[16] *BABAR* Collaboration, B. Aubert *et al.*, Phys. Rev. **D71**, 091104 (2005);